arXiv:1701.01424v2 [cond-mat.stat-mech] 6 Jan 2017

Temperature-abnormal diffusivity in underdamped space-periodic systems driven by external time-periodic force

I.G. Marchenko
NSC "Kharkov Institute of Physics and Technology", 1 Akademicheskaya str., Kharkov 61108, Ukraine and Kharkov National University, 4 Svobody Sq., Kharkov 61077, Ukraine

I.I. Marchenko
NTU "Kharkov Polytechnic Institute", 21 Frunze str., Kharkov 61145, Ukraine

A.V. Zhiglo*
NSC "Kharkov Institute of Physics and Technology", 1 Akademicheskaya str., Kharkov 61108, Ukraine and Kavli Institute for the Physics and Mathematics of the Universe (WPI), The University of Tokyo, Kashiwa, Chiba 277-8583, Japan

(Dated: January 9, 2017)

We present a study of diffusion enhancement of underdamped Brownian particles in 1D symmetric space-periodic potential due to external symmetric time-periodic forcing with zero mean. We show that the diffusivity can be enhanced by many orders of magnitude at appropriate choice of the forcing amplitude and frequency. The diffusivity demonstrates TAD, abnormal (decreasing) temperature dependence at forcing amplitudes exceeding certain value. At any fixed forcing frequency Ω normal temperature dependence of the diffusivity is restored at low enough temperatures, $T < T_{\rm TAD}(\Omega)$ — in contrast with the problem with constant external forcing. At fixed temperature at small forcing frequency the diffusivity either slowly decreases with Ω, or (at stronger forcing) goes through a maximum near Ω_2, reciprocal superdiffusion stage duration. At high frequencies, between Ω_2 and a fraction of the oscillation frequency at the potential minimum, the diffusivity is shown to decrease with Ω according to a power law, with exponent related to the transient superdiffusion exponent. This behavior is found similar for the cases of sinusoidal in time and piecewise constant periodic ("square") forcing.

PACS numbers: 05.40.-a, 02.50.Ey, 68.43.Jk, 66.30.J-

I. INTRODUCTION

The phenomena of diffusion and transport over a potential energy landscape play a key role in a number of processes in physics, chemistry and biology [1–5]. Josephson tunneling junctions, superionic conductors, phase-locked-loop frequency control systems, charge density waves are a few examples of systems in which these processes in periodic potential are important [6].

In recent years the interest has been growing to experimental studies of manipulating the particle diffusion by external fields. One can effectively control the diffusion processes by varying the field parameters. For instance, huge enhancement in diffusivity (exceeding its value in the same system without extra forcing by a factor of order hundreds) was observed in studying particle diffusion in colloids with optical traps (optical vortices) [7]. Large increase in diffusivity was also observed in studies of paramagnetic particle diffusion on surfaces of garnet ferrites influenced by external time-periodic magnetic field [8]. In the same manner diffusivity growth with shaking strength was noticed in experiments with granular gas [9]. It turned possible to increase the diffusivity of ions in membrane channels by varying the external electromagnetic field [10]. One can increase the rates of diffusion-limited physical processes, and effectively separate micro- and nano-particles of different nature by varying diffusion coefficients in different directions [11].

Despite these remarkable achievements, quantitative description of such enhanced diffusion under the influence of external forces remains fragmentary to date.

A. Diffusion of Brownian particles in spatially-periodic potentials under constant external forcing

Special cases of underdamped and overdamped physical systems are often considered. In overdamped systems inertial effects may be neglected, significantly simplifying the mathematical treatment of the problem. In underdamped systems on the other hand the viscous decay of oscillations occurs on times long compared with the oscillation period in the potential; such systems are harder to investigate, and the progress in studying these is more limited compared with overdamped ones.

First detailed studies of a Brownian particle motion in a washboard potential (*i.e.* a periodic potential tilted

* azhiglo@uchicago.edu

with an additional constant force field) were carried out by H. Risken and colleagues [12, 13], for all values of the friction. It was shown that at low friction the appearance of "locked" (in which the particle oscillates around one minimum of the potential) and "running" (where the particle travels through many potential periods, not getting trapped at separate minima) solutions was important for the particle ensemble behavior. At small temperatures running solutions appear abruptly at the external force value exceeding certain critical $F_{\rm cr}$; at smaller forces a single class of solutions (locked) is realized. Systematization of the results of these studies may be found in authoritative monograph [6].

Approximate solution of the Fokker-Planck equation (FPE) for the coordinate and velocity distribution function was the central moment of these studies. Two different approaches were used, that were checked to produce compatible results.

In the first of these [12] by expanding the distribution function in Hermite functions in velocity and Fourier-series in space coordinate, the Fokker-Planck equation was transformed into an infinite set of coupled equations for the expansion coefficients. These equations were solved by a matrix continued fraction method. Particle flux was then expressed through the expansion coefficients, after appropriate series truncation. At smaller friction progressively more terms must be kept, making this method less efficient.

Another approach [13] is best suited for low friction, when the energy becomes a slow variable (changing on friction dissipation timescales). The distribution function was rewritten in the energy and configuration space coordinate variables, FPE was solved in these new variables with the help of physically-motivated self-consistent ansatz.

Many illuminating results were obtained for the distribution functions at various parameter values, stability domains of locked and running solutions, plots of the mean particle velocity, etc. Diffusion properties however remained not studied. This matter was partly addressed in other works, based on simulations of the stochastic Langevin equation.

Early systematic study of diffusion by means of numerical simulation of the Langevin equation in periodic potential with extra constant forcing was undertaken in [14] (similar simulations were reported in [15] for forcing with a time-periodic component). Costantini & Marchesoni analyzed both overdamped and underdamped settings. At low dissipation they observed significant enhancement of the spatial diffusion near the critical force $F_{\rm cr}$ ([14], Fig. 1: diffusivity ten times larger than its post-maximum value at $F = 2F_{\rm cr}$, at the temperature equal to 0.6 of the potential well depth U_0), and related that to features of the particle jump statistics and locked-to-running transition.

Further progress in studies of the diffusion under the action of constant force was made in [16–18]. Time-dependence of the particle ensemble dispersion was studied in [16]. It was shown for the first time that in underdamped systems a special regime of dispersionless transport was realized, in which dispersion virtually does not change with time, on certain limited interval of time. The authors explained this phenomenon, they showed that strongly non-equilibrium distribution of particles in space (with steep front and exponential tail; formed as the particles first exit their original potential well) persists for long times, before eventually broadening and assuming normal Gaussian shape.

The temperature dependence of the diffusivity was studied as well [18]. The authors observed that the maximal diffusivity $D_{\rm max}$ was achieved near the $F_{\rm cr}$. At low friction $D_{\rm max}$ was shown to depend abnormally on the temperature — increase with decreasing temperature T. Fitting (for the three temperatures studied) yielded $D_{\rm max} \propto T^{-3.5}$ relation.

The presence of such abnormal temperature dependence is one important aspect in which underdamped systems differ from overdamped ones. In fact, certain peculiarities in diffusivity at low temperatures are observed (for driven Brownian particles in space-periodic potentials) in overdamped situation as well. P. Reimann and colleagues [19] showed analytically that for a sinusoidal in space potential at external constant force value near F_0, the value required for direct particle pull over the potential barrier (Eq. 4 below, p. 4), the ratio of $D_{\rm max}$ to the diffusivity value D_0 in the viscous medium without lattice and bias forces grows at temperature decreasing $\propto T^{-2/3}$. Yet the diffusivity itself still vanishes at $T \to 0$, as $D_{\rm max} \propto T^{1/3}$ [19], and grows monotonically for all T.

Regions with $\partial D/\partial T < 0$ were obtained in overdamped problem in [20] (cf. Fig. 6) for specially crafted exotic potential, flat apart from narrow peaks. The authors linked this abnormal diffusivity behavior to the large ratio of relaxation to escape time in such a system. Similar abnormal $D(T)$ behavior was found in [21] (cf. Fig. 2–4) for piecewise linear potential at extreme asymmetry, essentially sawtooth. So, while possible at large friction, special atypical conditions must be met for existence of parameters $\{F, T\}$ at which $\partial D/\partial T < 0$. On the contrary, such parameters exist universally in the problem with small friction ([22], more below).

Another distinction of the diffusivity in overdamped problem is that the maximum in $D(F)$ is achieved close to the F_0. Whereas at low friction $D_{\rm max}(F)$ is achieved at (typically much smaller) $F_{\rm cr}$. Experimental data for diffusion of colloidal particles in a tilted potential created with laser traps [23], Fig. 1, agreed reasonably well with this analytic [19] $D(F)$ dependence. The potential barrier height and the free diffusion coefficient were treated as fit parameters. Similarly, diffusivity in [24] (Fig. 7) showed peaked at F_0 behavior, and agreed fairly well with analytic predictions from [19] with the potential form inferred from independent study of the colloidal particle spatial distribution function. In this work colloidal particles diffused over the potential created by the bottom grid of colloidal spheres, and extra constant forcing was

due to gravity (controlled by the sample inclination angle). Different limiting cases of analytic predictions [19] for the mean particle velocity and diffusivity were compared with experimental results at different settings, and showed good agreement.

The physical reason behind the abnormal temperature dependence of diffusivity in underdamped systems is traced to increasing jump length of running particles (before getting retrapped at another potential minimum) with the temperature decrease [22]. This phenomenon being absent in overdamped systems (as these have no proper running states). The maximal diffusivity is achieved at forcing near $F_{\rm cr}$, as at this value populations of locked and running particles are about equal, and it is the mutual motion between these two populations (with temperature-independent running particle speed) that leads to fast spreading of the particle packet, manifested as giant diffusion [18].

More thorough analysis of (the temperature- and force-dependence of) the diffusion in underdamped systems was carried out in [25]. It was shown by numeric simulations of the Langevin equation that the phenomenon of diffusivity growth with the temperature decreasing (in the current work called TAD, "temperature-abnormal diffusivity") was only manifested in a narrow interval of applied external forcing. Study in a wide range of temperatures demonstrated that the diffusivity grew with decreasing temperature as $D_{\max} \propto T^{2/3} \exp\left[\mathcal{E}/(k_B T)\right]$ for certain $\mathcal{E} > 0$, checked valid for $k_B T/U_0 \in [0.05; 0.85]$; whereas the power-law fit $D_{\max} \propto T^{-3.5}$ proposed in [18] could approximate the results only in the narrow temperature range studied by the authors. We showed that the main exponential growth resulted from such of the correlation time at the temperature decreasing (found from the simulation results).

The diffusion properties were further elucidated and systematized for a broad range of the forces F, friction coefficients γ and temperatures T in [22], in sinusoidal 1D potential in underdamped setting. We introduced a velocity potential $W(V)$, which in part governed time evolution of certain slow (not changing much on times of order one period $\widetilde{\mathcal{T}}_0$ of small oscillations in the potential, rather evolving on viscous dissipation timescales) velocity variable, defined through a discrete quantity, maximal velocity in such consecutive oscillations. With certain reservations that $W(V)$ also defined the velocity distribution function $N(V)$ agreeing well with the one found numerically. The latter showed clear bimodal structure with maxima at $V = 0$ (locked states) and $V = F/\gamma$ (running ones) at intermediate forcing values. In this region of forcing values TAD was observed.

Analytic expressions for the mean particle velocity $\langle V \rangle$ and diffusivity were obtained with the model $N(V)$, good agreement was shown with direct Langevin equation simulation results. Simple fits were proposed determining the model parameters [entering $W(V)$ and $N(V)$] through F and γ, which — apart from usefulness for experimentalists/applications — allowed one to comprehend the features of transport and diffusivity in all the physical parameter space. Physical reason for the $D_{\max} \propto \exp\left[\mathcal{E}/(k_B T)\right]$ scaling was explained. More detail in the introductory part of Sec. III, p. 5 below.

B. Periodic in time external forcing

In practical applications periodic in time external forces (electromagnetic, acoustic, etc.) are more straightforwardly realized than constant forcing. It is natural to study how the findings for the constant forcing problem are modified for the time-periodic forcing setup, both from theoretical and practical point of view. By changing the diffusivity with the aid of periodic external fields it is possible to create surface structures with prescribed properties; influence the dynamics of point defects, under irradiation in part; alter the dislocation motion dynamics; increase chemical reaction rates in selected directions; manipulate the efficiency of processes in biological systems, to mention just a few applications [26, 27].

Most of the works on periodic forcing deal with ratchet-type systems [4] or stochastic resonance. Studies focusing on diffusion properties are scarce. We are not aware of any works that systematically study the combined dependence of the diffusivity on the temperature, the forcing amplitude and frequency in a representatively broad range of these parameters.

Dependence of the diffusivity on the interplay between the external periodic (piecewise constant, Eq. 6 on p. 4 below) forcing and the lattice force was studied in [28] in 2D overdamped setup. The forcing frequency was fixed at one value. It was shown that in a system with a sum of Yukawa potentials at square grid nodes the particle diffusivity was significantly enhanced for certain intricate set of bands ("A-windows") of the forcing amplitudes and orientations with respect to the grid. At special forcing arrangement TAD was observed for some diffusivity tensor components, and one of its principal values increased exponentially with inverse temperature. The other diffusivity tensor principal value decreased exponentially at the same time. It is likely that multi-dimensionality effects were crucial for TAD. Instead of having two, locked and running, populations in 1D accounting for (already sophisticated in this case) diffusion features, flows in higher dimensional problems are far more complex, known to result in further peculiarities in transport and diffusion [5, 29].

Underdamped 1D system was studied in [30], with a sinusoidal potential (same as Eq. 3 below) and sinusoidal in time forcing. Diffusivity enhancement by orders of magnitude was seen. TAD was observed for some (low) forcing frequencies, at the forcing amplitude $0.15F_0$ studied. Dependence of the diffusivity on the forcing frequency was studied in more detail in [31], and was shown to be nonmonotonic at large forcing amplitudes ($0.15F_0$ and $0.25F_0$, at $T = 240$ K, $k_B T/U_0 = 0.258$.) At $0.15F_0$ the maximum in the frequency dependence of the dif-

fusivity $D(\Omega)|_{\{T,F\}=const}$ persisted for all the temperatures studied, corresponding frequency $\Omega_{\max}$ increasing from $\sim 2\times10^{-4}$ to $\sim 6\times10^{-3}$ (in units of the potential eigenfrequency) at T varying from 120 to 360 K, $k_BT/U_0 \in [0.129; 0.388]$.

The goal of the present work is to investigate in detail the dependence of the diffusivity on the amplitude and the frequency of uniform time-periodic external forcing in a 1D underdamped space-periodic system, and conditions under which TAD is realized. We mainly study piecewise constant periodic (PCP: Eq. 6) forcing as this case is more straightforward to relate to the results for constant forcing.

The equations solved and the methods used are described in Sec. II. In Sec. III we show how the diffusivity changes with the PCP forcing frequency Ω, starting from the understood results at constant forcing, $\Omega = 0$. We observe that TAD is realized for some (intermediate) forcing amplitudes. Sec. IV is devoted to studying the $D(T)$ behavior at fixed Ω. The results for the diffusivity in the case of sinusoidal in time forcing are shown in Sec. V. We conclude in Sec. VI.

II. PROBLEM SETUP AND NUMERICAL METHOD

A. Problem setup

In this paper the 1D dynamics of a particle subject to external forcing F_t is described by the Langevin equation:

$$m\ddot{x} = -dU(x)/dx - \gamma\dot{x} + F_t(t) + \xi(t), \tag{1}$$

where t is the time, x is the particle coordinate, m is its mass, γ is the friction coefficient. Overdot stands for time differentiation. $\xi(t)$ represents thermal fluctuations, described by Gaussian white noise with correlation

$$\langle\xi(t)\xi(t')\rangle = 2\gamma k_BT\delta(t-t');\ \langle\xi(t)\rangle = 0. \tag{2}$$

Here k_B is the Boltzmann constant, T is the temperature.

The potential energy $U(x)$ is taken

$$U(x) = -(U_0/2)\cos(2\pi x/a), \tag{3}$$

where a is the lattice constant and U_0 is the potential barrier height.

The lattice force $F_{\rm lat}$ acting upon the particle is

$$F_{\rm lat}(x) = -dU/dx = -F_0\sin(2\pi x/a). \tag{4}$$

Quantity $F_0 = \pi U_0/a$ corresponds to the minimal external force needed to drag the particle over the potential barrier separating potential minima on the 1D lattice at large friction.

We use the same physical parameters as in [22], typical for adatom diffusion on close-packed metal surfaces. Namely, values

$$U_0 = 80 \text{ meV}, a = 2 \text{ Å} \tag{5}$$

for the activation barrier and the lattice constant are adopted.

Two possibilities for the external periodic forcing are studied: piecewise constant periodic (**PCP**) driving

$$F_t(t) = F_e\,\mathrm{sign}[\sin(\Omega t)] \tag{6}$$

and sinusoidal one,

$$F_t(t) = F_e\sin(\Omega t). \tag{7}$$

Ω is the angular frequency of the external force and F_e is its amplitude.

It is convenient to use dimensionless time t' and space coordinate x', normalizing the physical values to the period of small oscillations $\mathcal{T}_0 \equiv 2\pi/\Omega_0 = a(2m/U_0)^{1/2}$ at the potential minimum in the absence of friction, and to the lattice spatial period a respectively:

$$t' = \frac{t}{\mathcal{T}_0} = \frac{t}{a}\sqrt{\frac{U_0}{2m}},\quad x' = \frac{x}{a}. \tag{8}$$

Dimensionless temperature T' and friction coefficient γ' are further introduced:

$$T' = 2k_BT/U_0,\ \gamma' = \gamma a(mU_0/2)^{-1/2}. \tag{9}$$

Definitions (8,9) differ from such in [16, 22, 25, 30–32] by extra factors of 2 appearing in the definition of t', and consequently in T' and γ' as well. Current definition makes interpreting the results easier ($t' = 1$ corresponds to one oscillation period at small γ'). For more straightforward comparison with our previous works we also use another dimensionless temperature in the figures,

$$T^\dagger = k_BT/U_0 = T'/2.$$

The parameters of the dimensionless problem are F_e/F_0, $\omega = \Omega\mathcal{T}_0$, γ', T'. In the new variables the equation of motion has form Eq. 1 with unit new mass, potential $\cos(2\pi x')$ with no prefactors and the external forcing amplitude made dimensionless with a $2a/U_0$ multiplier.

Below lowercase ω's (frequencies), and corresponding periods $\tau = 2\pi/\omega$ denote dimensionless quantities. Physical frequencies and periods are obtained by respectively dividing and multiplying these by the the period $\mathcal{T}_0$ of small oscillations in the lattice potential at $\gamma = 0$.

Overdamped problem is characterized by $\gamma/m \gg \Omega_0$, whereas $\gamma/m \ll \Omega_0$ (equivalently, $\gamma' \ll 1$) corresponds to underdamped dynamics. We study the underdamped case here. Friction coefficient $\gamma' = 0.2$ we use corresponds to the same physical value as in earlier studies [22, 25].

B. Numerical method

We solve stochastic equation (1,2) numerically using a Verlet-type algorithm [33] with a time step Δt somewhat shorter than $1/100^{\rm th}$ of the period of oscillation $\mathcal{T}_0$. The

statistic averaging is performed over the ensemble consisting of at least $N = 5 \times 10^4$ particles. To verify the modeling consistency some computations were performed with $N = 5 \times 10^6$.

The initial conditions are set as follows. Each particle is placed at $x = 0$, its velocity chosen at random, with Maxwellian distribution for a given T. Thermalization over 100 oscillation periods, in the potential $U(x)$ but without the $F_t(t)$, is then used to get equilibrium particle distribution over both coordinate and velocity. Tests show that the distribution function does not change after that time. In the process of such thermalization the particles can jump to nearby elementary cells of the lattice. Such relocated particles are returned back to the initial cell by translation over an integer multiple of the lattice constant, to get diffusion of all particles starting from the initial cell of the lattice.

The diffusivity is computed based on the dispersion σ^2 of the particle distribution in the limit of large times:

$$D' = \lim_{t\to\infty} D'_{\rm eff}(t) = \lim_{t'\to\infty} \frac{\langle (x' - \langle x' \rangle)^2 \rangle (t')}{2t'} \equiv \lim_{t'\to\infty} \frac{\sigma^2}{2t'}. \quad (10)$$

Angle brackets $\langle \ldots \rangle$ with no subscripts mean averaging over the ensemble. D' and σ are dimensionless in our notation. The physical diffusivity is $D = D' a^2/\mathcal{T}_0$.

For each diffusivity calculation we find time $t'_{\rm lin}$, after which the dispersion grows linearly with time (if averaged over the forcing period). The D' is calculated as $\sigma^2/(2t')$ at $t' = 100 t'_{\rm lin}$.

It is known that in systems with low dissipation transient regimes of anomalous diffusion can be realized [32], characterized by

$$\sigma^2 = \langle (x' - \langle x' \rangle)^2 \rangle \propto t'^{\alpha}. \quad (11)$$

The process with $\alpha > 1$ is referred to as superdiffusion, whereas subdiffusion is characterized by $\alpha < 1$. Stages of anomalous diffusion were observed in our simulations. The choice of initial conditions above aided in having these stages in clear form.

We determine the exponents α by the least-square linear fitting between $\log(\sigma^2)$ and $\log t$ on the time-interval of interest.

III. PIECEWISE CONSTANT PERIODIC FORCING. DEPENDENCE OF THE DIFFUSIVITY ON THE FORCING FREQUENCY

In [25] it was shown that depending on the value of the external force (constant in that study) different functional dependences of the diffusivity on the temperature were realized.

Plots of the diffusivity as a function of the external force at several temperatures (based on [25], recomputed for the current units) are shown in Fig. 1. There are three regions of F_e values (I–III), with qualitatively different dependence of the diffusivity D on T. In region I diffusion is enhanced as external force F_e value increases, whereas in region III diffusion is inhibited as F_e increases. In regions I and III D grows with T increasing. Contrary to this (normal temperature behavior) in region II D grows as T decreases. This is the region of "temperature-abnormal diffusivity" (TAD). The *diffusion process* at sufficiently late times is normal, $\sigma^2 \propto t^1$, however the *diffusion coefficient* $D' = \sigma^2/(2t')$ (abnormally) increases as the temperature decreases.

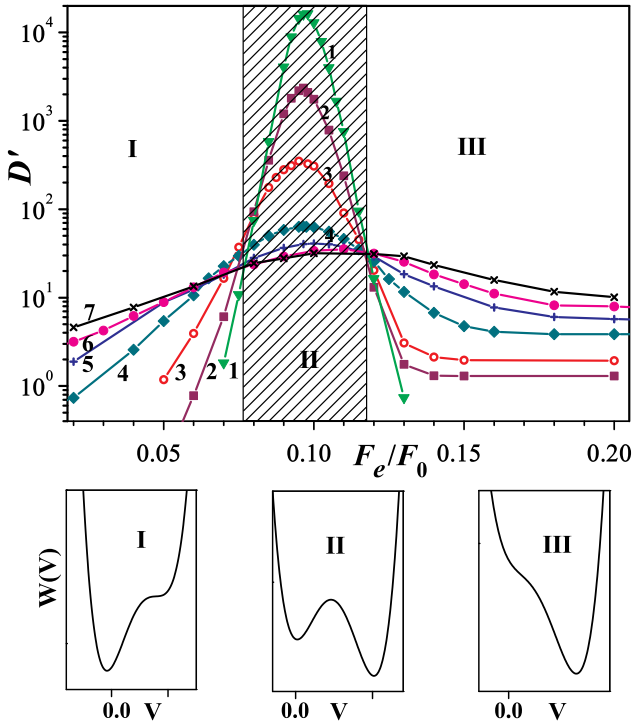

FIG. 1. (Color online) Dependence of the dimensionless diffusivity on the external constant forcing at different temperatures (top). The region of anomalous temperature dependence (II) is hatched. The friction coefficient $\gamma' = 0.2$. 1: $T^\dagger = 0.097$ [$T = 90$ K for the potential characteristic of the H-adatom diffusion on metal surface (5)], 2: $T^\dagger = 0.129$, 3: $T^\dagger = 0.194$, 4: $T^\dagger = 0.388$, 5: $T^\dagger = 0.582$, 6: $T^\dagger = 0.776$, 7: $T^\dagger = 0.969$.
Bottom: the effective velocity potential in the three force regions.Left, middle and right diagrams correspond to $F_e/F_0 =$ 0.06, 0.095 and 0.25 respectively.

In [30] it was seen that TAD is also possible at time-periodic external forcing. At such forcing TAD was only observed in a limited interval of the forcing frequencies. Studies were carried out at $F_e = 0.15 F_0$, that would correspond to region III for the same amplitude of constant forcing (see Fig. 1), so TAD would not be observed at such F_e value were the forcing $F_t(t)$ constant.

To understand physical reasons of the abnormal temperature dependence of the diffusivity in these two different (time-periodic, and constant) forcing regimes we consider the periodic forcing regime in more detail below. For piecewise constant periodic (PCP) forcing one

can use intuition gained in the constant forcing problem for the time intervals in which F_t stays constant, the findings are thus easier to interpret. Most of the results in this work are for the PCP forcing setup.

In [22] we showed that the transport properties of an ensemble of underdamped particles in a washboard potential can be found by considering a simpler problem of the overdamped motion in effective potential $W(V)$ in velocity space. The problem showed similarities with the problem of active Brownian particle motion [34]. Whether the particle belongs to locked [tending with time to $V = 0$, one minimum of $W(V)$] or running [tending to $V = F/\gamma$, another minimum of the asymmetric double-well potential $W(V)$] population in the absence of noise is determined by the particle's initial state (its velocity, if placed at the potential minimum at $t = 0$). It was shown that region II of the force values, the region in which TAD is observed, is precisely the region where both locked and running solutions are simultaneously possible.

The $W(V)$ was also instrumental for proposing a model distribution function $N(V)$, and for defining diffusivity through Kubo relation. The analytic predictions for D and $\langle V\rangle$ based on the model $N(V)$ agreed well with direct numerical simulation results for all values of $F \lesssim 0.5F_0$, temperatures in the range $T^\dagger \in [0.129; 0.776]$, friction $\gamma' \in [0.1; 0.4]$ (in the definitions of dimensionless quantities adopted here, Eqs. (8,9); agreement getting progressively better at smaller γ'). In the expression for the diffusivity, (the analytic prediction for) the correlation time τ_{corl} factor was shown to be responsible for the main features in $D(F, T)$ dependence, numerically found in earlier study [25]. Namely, τ_{corl} showed proper nonmonotonic dependence on F, with a maximum near $F_{\rm cr}$, progressively more pronounced at smaller T. τ_{corl} increased at temperature decreasing $\propto \exp[\mathcal{E}/(k_BT)]$ (for certain $\mathcal{E} > 0$); this increase at low T reflected the Kramers rate for transitions in the double-well velocity potential $W(V)$, between the wells corresponding to locked and running states.

Schematics of the effective velocity potential in the three regions of the applied force are shown in the bottom insets in Fig. 1. The first inset corresponds to $F_e = 0.06F_0$, at which only locked solutions exist. In the second inset $F_e = 0.095F_0$, corresponding to the maximal diffusivity; both types of solutions coexist at this force value. Finally $F_e = 0.25F_0$ corresponding to region III is shown in the third inset; at this F_e only running solutions are realized. The boundaries between regions I–III depend on γ and m (on γ' in the dimensionless problem). At smaller γ' these boundaries move to the left, to the lower force values, and the width of region II decreases. In the current study we use the same fixed values of γ and m as in [22], and investigate the features of $D(T|\omega)$ at the three values of the external forcing amplitude listed above.

It may be expected that the same picture for different temperature behaviors of the diffusivity, with analogous three regions I–III of the external force amplitudes, holds for PCP driving, at least at small frequencies Ω. The description with the effective potential is applicable, the potential $W(V)$ keeping constant form for each of the two half-periods of the external forcing [on which F_t stays constant, this F value defining corresponding $W(V|F, \gamma)$.]

Below we show that in fact the situation is more subtle. Similar three regions of the external force amplitudes F_e exist, differing in qualitative $D(T)$ dependence. TAD is realized in certain range of intermediate F_e, smoothly dependent on Ω. At decreasing temperatures the dependence $D(T)$ starts progressively deviating from such at constant forcing. For any fixed Ω at temperatures below certain critical $T_{\rm TAD}(\Omega)$, normal temperature dependence of the diffusivity is restored. We demonstrate these features by analyzing $D(T|\omega)$ in sequence for the above values of F_e ($F_e/F_0 = 0.06$, 0.095, 0.25), that correspond to regions I, II, III in the constant external force problem.

We observe transient anomalous diffusion phase, and see how its characteristics relate to the diffusivity in the asymptotic late time regime, when normal diffusion regime sets in. The properties of this anomalous diffusion stage are different in the three regions of the applied force amplitudes; this translates into different functional dependence of the diffusivity on the temperature.

A. Region I: $F_e/F_0 = 0.06$, varying frequency

Here we investigate how the diffusivity changes with (dimensionless) frequency $\omega = \Omega\mathcal{T}_0$ of the external forcing at forcing amplitude $F_e = 0.06F_0$. We show that the diffusivity stays nearly constant at small frequencies, up to reciprocal of the superdiffusion stage duration. At frequencies above this the diffusivity drops according to a power-law with exponent related to the exponent of the superdiffusion. This power-law dependence holds up to frequencies a few times less than the lattice potential eigenfrequency. The diffusivity grows with the temperature (normal temperature behavior), related to the superdiffusion stage duration increasing with T.

Figure 2 shows the growth of the particle dispersion with time. At constant external forcing this growth demonstrates a clear superdiffusion stage, $\sigma^2 \propto t'^\alpha$, $\alpha > 1$, that switches to normal diffusion (same power-law growth but with $\alpha = 1$) after certain time τ_2. The τ_2 as well as the superdiffusion exponent α depend on F_e/F_0 and other problem parameters, γ' and T'. For the values used $\tau_2 \approx 100$, $\alpha \approx 2.3$. Lowercase τ's everywhere are dimensionless, normalized to the period of small oscillations at the lattice potential minimum at $\gamma' = 0$,

$$\mathcal{T}_0 = 2\pi/\Omega_0 = a\sqrt{2m/U_0}. \tag{12}$$

σ^2 and D' are dimensionless dispersion and diffusivity.

Curves 1–3 correspond to three different frequencies. Oscillations in $\sigma^2(t')$ are clearly seen with double forcing frequency, 2ω. These are particularly large at ω around

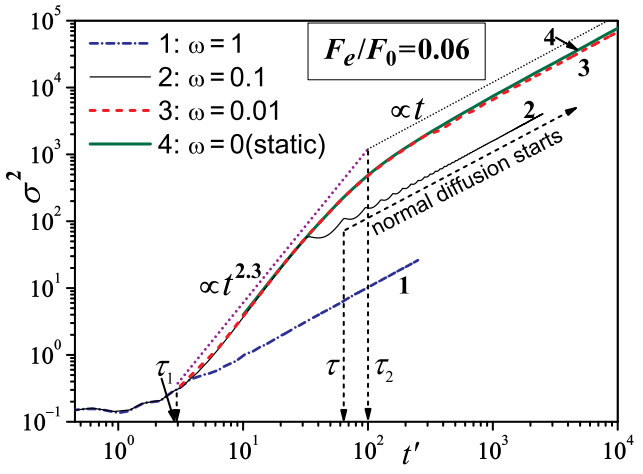

FIG. 2. (Color online) Time dependence of the dimensionless dispersion for the force value $F_e = 0.06F_0$ (region I) for different force frequencies. τ_2 denotes the end of the superdiffusion stage at constant forcing. $\tau = 2\pi/\omega$ is the period of the external periodic forcing. $T^\dagger = 0.194$. 1: $\omega = 1$, 2: $\omega = 10^{-1}$, 3: $\omega = 10^{-2}$, 4: $\omega = 0$ (constant external force.) Straight dashed and dotted lines show the power-law fitting behavior of the dispersion.

$\omega_2 = 2\pi/\tau_2$ (curve 2). At these values, interestingly, intervals of $\sigma^2(t)$ decreasing with time are observed. This effect can be seen in earlier works [35].

At frequencies below $\omega_2 = 2\pi/\tau_2$ the curves $\sigma^2(t)$ closely follow that at $\omega = 0$ (constant external force, curve 4). At higher frequencies the superdiffusion phase effectively ends after one period τ of the external force, normal diffusion sets in (in a sense that averaged over the forcing period $\langle d(\sigma^2)/dt\rangle_t \approx const$). Higher frequencies of the forcing correspondingly result in lower diffusivity, as the stage of σ^2 growing with time faster than linearly ends earlier than at lower ω's.

These results suggest the following approximations for the smoothed over the forcing period dispersion $\overline{\sigma^2}(t')$, valid not too close to the transition moments between different diffusion regimes:

$$\ln\frac{\overline{\sigma^2}}{\sigma_0^2} = \begin{cases} \approx 0 & \text{at } t' < \tau_1 \\ \alpha\ln(t'/\tau_1) & \text{at } t' \in (\tau_1;\tau_{2,\omega}) \\ \alpha\ln(\tau_{2,\omega}/\tau_1) + \ln(t'/\tau_{2,\omega}) & \text{at } t' > \tau_{2,\omega}. \end{cases} \quad (13)$$

Here $\sigma_0^2 = \sigma^2|_{t=0}$ (for the approximately Boltzmannian initial distribution of the particles in $x' \in (-0.5; 0.5)$ well of the potential), $\tau_{2,\omega} = \min(\tau_2, \tau)$, τ_1 is close to the first potential well exit time. Constants are chosen in such a way that the spline approximation (13) is continuous. Quantities α, $\tau_{1,2}$ depend on the problem parameters, T', F_e/F_0 and γ'. At fixed values of these parameters, the last approximation yields the dependence of the diffusivity $D' = \lim_{t'\to\infty} \sigma^2/(2t')$ on the forcing period τ

$$D'(\tau) = \begin{cases} (1/2)\sigma_0^2\tau_1^{-\alpha}\tau^{\alpha-1} & \text{at } \tau_1 < \tau < \tau_2 \\ (1/2)\sigma_0^2\tau_1^{-\alpha}\tau_2^{\alpha-1} & \text{at } \tau > \tau_2, \end{cases} \quad (14)$$

or on its frequency $\omega = 2\pi/\tau$

$$\frac{D'(\omega)}{D'(0)} = \begin{cases} 1 & \text{at } \omega < \omega_2 \\ (\omega/\omega_2)^{1-\alpha} & \text{at } \omega_2 < \omega < 2\pi/\tau_1. \end{cases} \quad (15)$$

The diffusivity thus should stay about constant at $\omega < \omega_2$, and at larger forcing frequencies drop with ω according to the power law, with exponent equal to $1 - \alpha$, determined by the superdiffusion exponent.

Figure 3 shows simulation results for $D'(\omega)$. Dotted lines show approximations Eq. 15. Dashed lines show the diffusivity at constant forcing with the same F_e value. These results confirm the features suggested by Eq. 15, away from transition frequency $\omega_2 = 2\pi/\tau_2$ and up to $\omega/2\pi \approx 0.1$. $D(\omega) < D(0)$ at any ω, and decreases with ω, up to the frequency values a few times smaller than the potential eigenfrequency.

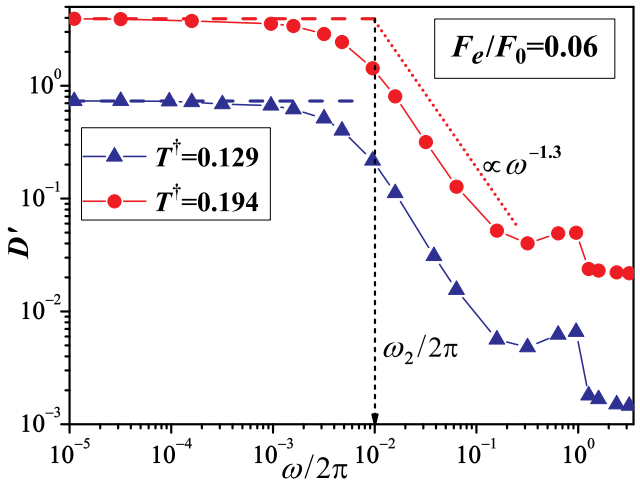

FIG. 3. (Color online) Dependence of diffusivity D' on the forcing frequency at $T^\dagger = 0.129$ (triangles) and 0.194 (circles). The dashed line asymptotes show the diffusivity values at constant forcing with the same $F_e/F_0 = 0.06$. The slanting dotted line shows the power law drop of D' at intermediate ω's.

Further ramification might have been added in Eqs. (13–15) for the case $\tau < \tau_1$, changing τ_1 to $\tau_{1,\omega} = \min(\tau_1, \tau)$; that would indeed lead to $D(\omega)$ increasing at $\omega > 2\pi/\tau_1$. With our parameters, however, resulting approximations are an overstretch; the diffusion gets markedly nonequilibrium at such high ω's, resulting in the complex $D(\omega)$ behavior at ω approaching 2π. More on this in Sec. III D.

Finally, Fig. 4 shows $\sigma^2(t)$ for a range of temperatures at constant forcing. Despite the superdiffusion exponent α is seen to decrease with the temperature, the duration

of the superdiffusion stage $\tau_{\rm spd} = \tau_2 - \tau_1$ grows fast with the temperature. As a result the dispersion is larger for larger temperatures at any given time. At late times this translates into diffusivity being larger at larger temperatures; so normal (increasing) $D(T)$ dependence is realized at force amplitudes in region I.

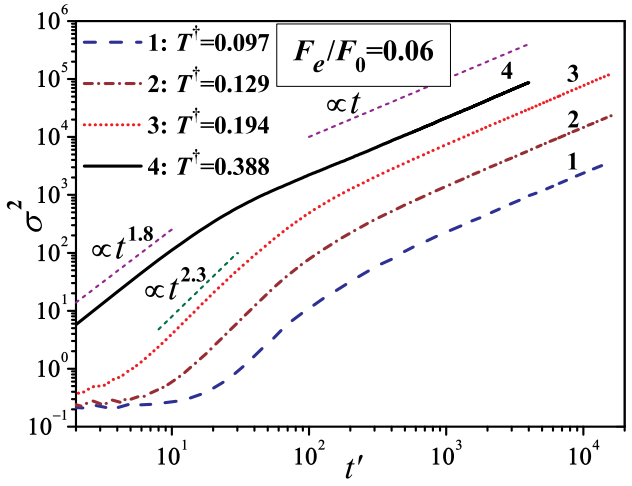

FIG. 4. (Color online) Dispersion variation with the temperature, at constant forcing ($\omega = 0$). 1: $T^\dagger = 0.097$, 2: $T^\dagger = 0.129$, 3: $T^\dagger = 0.194$, 4: $T^\dagger = 0.388$. The short-dashed straight lines show power-law fits for the transient superdiffusion stage, and the late-time normal diffusion regime.

B. Region II: $F_e/F_0 = 0.095$

Here we repeat analysis of the previous section for periodic forcing with amplitude $F_e = 0.095F_0$ (the value at which the maximal diffusivity is achieved at constant forcing). In the same manner as for the forcing amplitude in region I, transition from initial superdiffusion stage to normal diffusion at late times is observed, at time τ_2. At forcing frequency ω growing, the diffusivity again decreases only slightly from $D(\omega = 0)$ till ω reaches $\omega_2 = 2\pi/\tau_2$. It decreases fast, according to the same power law $D(\omega)/D(0) = (\omega/\omega_2)^{1-\alpha}$, at larger ω's, up to $1/\tau \approx 0.1$. Contrary to the case of weaker forcing considered in the previous section, superdiffusion duration $\tau_{\rm spd} = \tau_2 - \tau_1$ now *decreases* with the temperature. This leads to diffusivity growing at temperature decrease (TAD), at moderately low frequencies. This is the main effect we intended to find in the periodic driving setup, extending our previous findings at constant forcing [22].

Figure 5 shows growth of the particle dispersion with time. Again the superdiffusion stage is observed, and it ends after one period of PCP forcing or after τ_2 (the end time of superdiffusion at constant forcing), whichever is smaller. Thus the same approximations Eq. (13–15) are applicable for the (averaged over τ) dispersion growth $\overline{\sigma^2}(t')$ and dependence of the diffusivity on the forcing frequency $D'(\omega)$. Simulation results for $D'(\omega)$ (Fig. 6) again agree with prediction (Eq. 15).

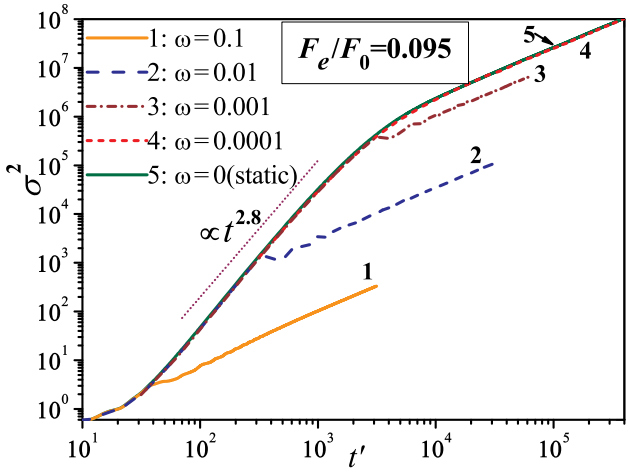

FIG. 5. (Color online) Time dependence of the dimensionless dispersion for the force value $F_e = 0.095F_0$ (region II) for different force frequencies. Curves 1–5, bottom to top: (dimensionless) $\omega = 10^{-1}$, 10^{-2}, 10^{-3}, 10^{-4}, 0 (constant forcing). $T^\dagger = 0.194$.

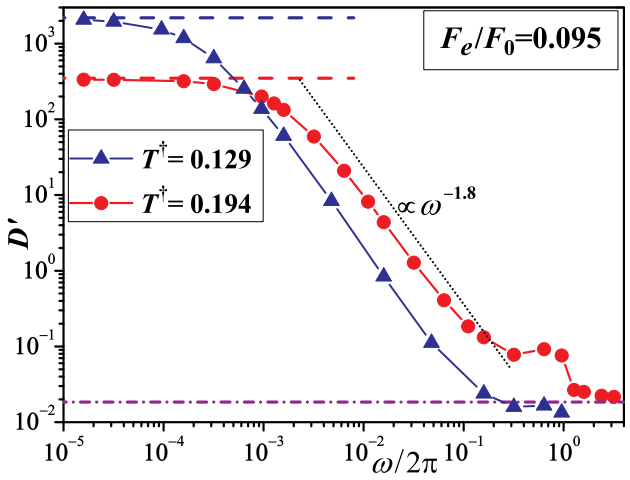

FIG. 6. (Color online) Dependence of diffusivity D' on the external force frequency ω, at $T^\dagger = 0.129$ (triangles) and 0.194 (circles). The dashed line asymptotes show the diffusivity values for constant forcing with the same $F_e/F_0 = 0.095$. Dotted line shows the power law drop of D' at higher ω's. The dot-dashed horizontal line asymptote (for high ω) is at the diffusivity value in the lattice periodic potential in the absence of extra driving, $F_t(t) = 0$, for $T^\dagger = 0.194$.

As $D(\omega)$ does not vary much at $\omega < \omega_2$, TAD must be observed at small frequencies, at it is observed at constant forcing ([22]: $D(F_e, \omega = 0)$ decreases with the temperature when F_e is in region II). Such an abnormal dependence on the temperature is due to longer jumps the

particles perform on average at lower temperatures. This in turn follows from lower probability at lower temperatures to turn the running particle into a locked state: such a transition requires certain threshold energy transfer to such a particle, and at lower temperatures the probability of such a transfer decreases exponentially with inverse temperature. Hence the running particle travels at about the stationary speed F_e/γ (the speed fluctuating around this average due to the lattice potential) for increasingly longer distances before getting trapped again in some next well of the potential, resulting in larger diffusivity at smaller temperatures. This mechanism is not applicable in region I, where only locked solutions are realized.

In terms of the dispersion evolution features, this phenomenon of the diffusivity growing at the temperature decreasing results from the superdiffusion duration $\tau_{\rm spd} = \tau_2 - \tau_1$ growing at temperature decreasing, as Fig. 7 demonstrates. This qualitatively differs from the situation at forcing amplitude in region I (end of the previous section). We note that α increases with the temperature decreasing, same as in region I.

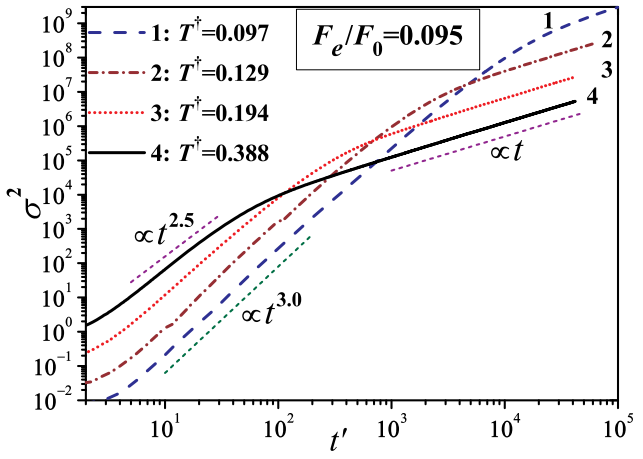

FIG. 7. (Color online) The dispersion variation with the temperature, at constant forcing ($\omega = 0$). 1: $T^\dagger = 0.097$, 2: $T^\dagger = 0.129$, 3: $T^\dagger = 0.194$, 4: $T^\dagger = 0.388$. $F_e/F_0 = 0.095$.

At higher frequencies, on the other hand, the diffusivity starts increasing with the temperature (normal behavior). This results from τ_2 decreasing with the temperature, as can be seen in Fig. 7. Despite $D(\omega = 0)$ is larger at smaller temperature T_1, as ω grows the $D(\omega\,|T_1)$ starts decreasing according to the power law earlier [at ω's near the smaller $\omega_2 = 2\pi/\tau_2(T_1)$] than $D(\omega\,|T_2)$ for $T_2 > T_1$ does. And the exponent of this power-law decreases with T decreasing, $1 - \alpha(T_1) < 1 - \alpha(T_2) < 0$ — therefore at larger frequencies, commensurate with ω_2, the diffusivity starts increasing with the temperature, *TAD disappears*.

As it is the case for the forcing amplitude in region I, $D(\omega)$ decreases monotonically with ω from $D(0)$, up to the frequency values $\omega \approx 0.3 \times 2\pi$ (at frequencies so high the particle transport becomes substantially non-equilibrium, that affecting the functional dependence $D(\omega)$, as discussed in Sec. III D below).

C. Region III: $F_e/F_0 = 0.25$

For strong forcing (region III, in which the diffusivity decreases with F_e in constant forcing setup, and increases with the temperature) we demonstrate in this subsection that the dependence of dispersion on time shows new features. After initial superdiffusion stage at times $t' < \tau_2$, prolonged dispersionless stage sets in, till $\tau_3 \sim 10^3\tau_2$. In this stage the dispersion stays nearly constant. As at weaker external forcing (regions I, II), both these stages may be interrupted earlier in the case of high forcing frequency (after about a period of the forcing). At late times normal diffusion takes place. Dependence $D(\omega)$ is non-monotonic here, agreeing with findings in [30]. D reaches a maximum near $\omega = \omega_2 \equiv 2\pi/\tau_2$. TAD is observed at intermediate frequencies.

Figure 8 shows the particle dispersion as a function of time. At low frequencies of the forcing, superdiffusion is observed till $\tau_2 \approx 200$. Dispersionless stage is realized later, at $t' \in (\tau_2; \tau_3)$. Physically τ_2 is the time at which the particle distribution function in velocities assumes its stationary form. The distribution in space is still strongly non-equilibrium at τ_2, it has exponential tail and sharp front [16] (in the direction of F). It takes till τ_3 for the distribution function to assume approximately Gaussian shape in space (if averaged over the potential spatial period). On interval $(\tau_2; \tau_3)$ dispersion does not increase siubstantially. After τ_3 normal diffusion sets in, $\sigma^2/t' = 2D' + o(1)$ at $\tau_3 \ll t' \to \infty$.

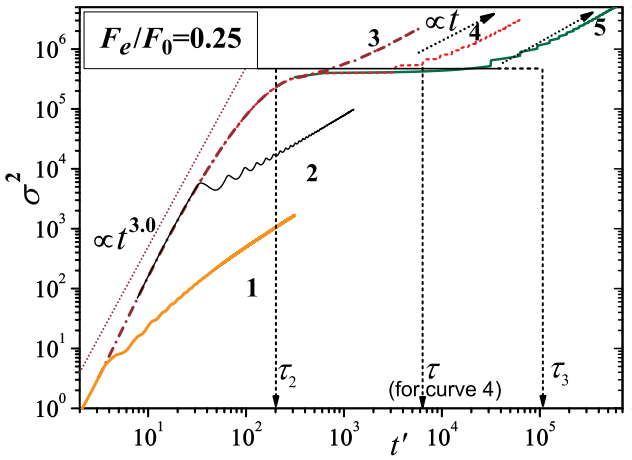

FIG. 8. (Color online) Time dependence of the dimensionless dispersion at $F_e = 0.25F_0$ (region III) for different force frequencies. Curves 1–5: (dimensionless) $\omega = 1$, 10^{-1}, 10^{-2}, 10^{-3}, 10^{-4}. $T^\dagger = 0.194$. Dotted lines show power-law fitting behavior of the dispersion.

The whole curve $\sigma^2(t')$ differs insignificantly from $\sigma^2(t')$ in constant forcing setup if the forcing frequency $\omega < \omega_3 \equiv 2\pi/\tau_3$. This $\sigma^2(t')$ dependence is modified at higher frequencies of the external forcing (in a similar way to the behavior discussed in Sec. III A–III B at weaker forcing). For $\omega \in (\omega_3;\omega_2)$ the dispersionless stage is interrupted after about one period of external force, after which time approximately linear dependence (if averaged over times $\sim 2\pi/\omega$) sets in, $\langle d\sigma^2/dt'\rangle_{t'} = 2D'$, D' equal to its asymptotic (at $t' \to \infty$) value. At yet higher forcing frequencies, $\omega > \omega_2$, dispersionless stage is not realized at all, normal diffusion sets in right after the prematurely interrupted superdiffusion stage.

Similarly to the previous sections, described above dependence of $\ln\overline{\sigma^2}$ on $\ln t'$ can be schematized by the following continuous piecewise linear approximation (meaningful not too close to switching time-points τ_{1-3}):

$$\ln\frac{\overline{\sigma^2}}{\sigma_0^2} = \begin{cases} \approx 0 & \text{at } t' < \tau_1 \\ \alpha\ln(t'/\tau_1) & \text{at } t' \in (\tau_1;\tau_{2,\omega}) \\ \alpha\ln(\tau_{2,\omega}/\tau_1) & \text{at } t' \in (\tau_{2,\omega};\tau_{3,\omega}) \\ \alpha\ln(\tau_{2,\omega}/\tau_1) + \ln(t'/\tau_{3,\omega}) & \text{at } t' > \tau_{3,\omega}. \end{cases} \tag{16}$$

Here $\tau_{3,\omega} = \min(\tau_3,\tau)$, $\tau_{2,\omega} = \min(\tau_2,\tau)$; $\tau > \tau_1$ assumed. As before, $D(\omega)$ can be found from this, showing the same power law decay as in Eq. 15 at $\omega > \omega_2$, and additional, linearly growing with ω feature at intermediate frequencies:

$$\frac{D(\omega)}{D(0)} = \begin{cases} 1 & \text{at } \omega < \omega_3 \\ \omega/\omega_3 & \text{at } \omega \in (\omega_3;\omega_2) \\ (\omega/\omega_2)^{1-\alpha}\omega_2/\omega_3 & \text{at } \omega > \omega_2. \end{cases} \tag{17}$$

Simulation results for $D(\omega)$ are shown in Fig. 9 for two temperatures. They indeed show the features suggested in Eq. 17. At high frequencies, $\omega > \omega_2$, the superdiffusion stage switches to normal diffusion earlier than at τ_2, at time $\sim \tau = 2\pi/\omega$. This behavior is the same as for the forcing amplitude in regions I–II. Thus in the same manner the diffusivity grows as ω decreases, as the longer interval (till $t' \approx \tau$) of superdiffusive dispersion growth is used at the forcing period τ getting longer. However at smaller frequencies, $\omega_3 < \omega < \omega_2$, it is the dispersionless phase that gets interrupted prematurely (*i.e.* it is not realized in full, till τ_3, as it would have at $\omega = 0$), so the earlier such a switch occurs (*i.e.* the shorter the τ), the higher diffusivity is obtained in the late-time normal diffusion stage. This explains the growth of $D(\omega)$ with ω at $\omega \in (\omega_3;\omega_2)$. The maximum in $D(\omega)$ is thus observed, at $\omega_{\max} \approx \omega_2$.

This differs from monotonically decreasing $D(\omega)$ in regions I, II. Such a nonmonotonic dependence $D(\omega)$ was observed in [30, 31]; the forcing studied was sinusoidal in time, its amplitude (indeed) corresponded to region III in terminology of this work.

$\omega_{\max}$ together with $2\pi/\tau_2$ increase with the temperature. The maximal value of the diffusivity (achieved at $\omega_{\max}$) increases as the temperature decreases, due to the dispersionless stage duration $\tau_3 - \tau_2$ growing fast at temperature decreasing. And so does $D(\omega)$ at a given ω near ω_2 in a limited range of temperatures. So abnormal temperature dependence of the diffusivity (TAD) is realized in intermediate region of the forcing frequencies around ω_2. The temperature dependence of the diffusivity is studied in more detail in Sec. IV below.

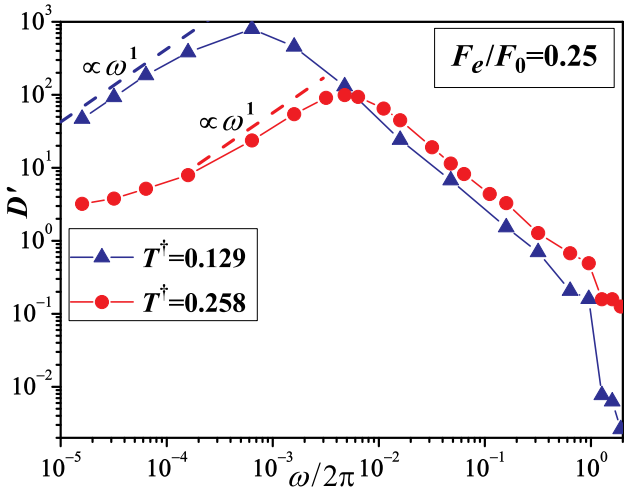

FIG. 9. (Color online) Dependence of the dimensionless diffusivity D' on the forcing frequency, at $T^\dagger = 0.129$ (circles) and 0.194 (triangles). The dashed lines show approximately linear growth at $\omega \in (\omega_2;\omega_3)$.

D. Diffusivity at high forcing frequency ω

As the simulation results suggest, the power law decay of $D(\omega)$ at large ω's (Figs. 3, 6, 9) does not hold at frequencies that are too high, above $\sim 1/10^{\text{th}}$ of the eigenfrequency at the lattice potential minima. This is due to the diffusion process becoming markedly nonequilibrium. The distribution function in velocities differs significantly from such at constant forcing at all times; description in terms of the velocity potential $W(V)$ is no longer useful.

To analyze this we introduce kinetic temperature $T^* = m\langle\Delta v^2\rangle/U_0$ (*i.e.*, made dimensionless with the same multiplier k_B/U_0 as $T^\dagger$), and study its evolution at different ω's: Fig. 10, bottom. At low frequency, T^* does not change (only shows random noise) after one period $\tau = 2\pi/\omega$ of the forcing. At larger $\omega = 2$ regular oscillations in T^* are observed at all times, with amplitude of order 5% of the average T^* value. That average is about 10% higher than the average T^* at $\omega = 10^{-2}$. T^* averaged over the forcing oscillation period grows for about $t'_{\text{st}} \approx 7\tau$ until it reaches its stationary value.

Together with T^*, $\sigma^2(t')$ also shows transient behavior at $t' < 7\tau$. We illustrate this in the top graphs in Fig. 10,

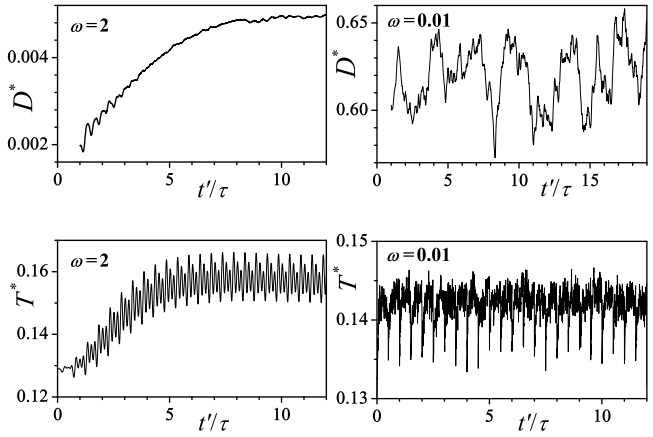

FIG. 10. Evolution of the diffusivity and the kinetic temperature for high and small frequencies of the forcing, $\omega = 2$ and 10^{-2}. $F_e/F_0 = 0.06$. Note that time normalized to one *forcing* period τ (rather than to $\mathcal{T}_0$ as in the previous t-dependence graphs) is shown along the abscissa axis.

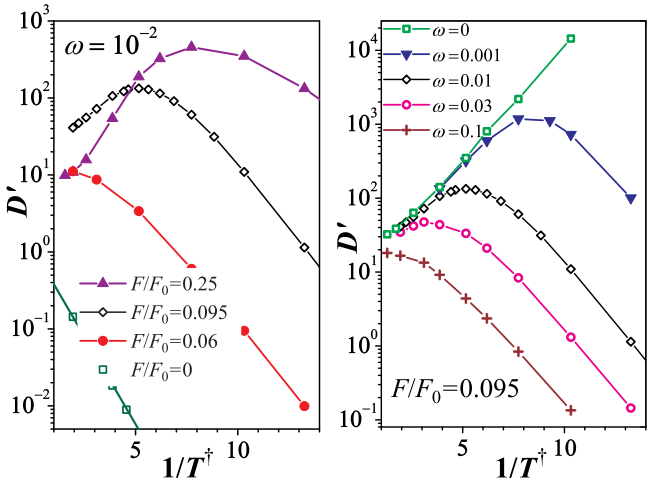

FIG. 11. (Color online) Dimensionless diffusivity vs $1/T$ at (left): $\omega = 10^{-2}$, force amplitudes $F_e/F_0 = 0$ (squares, and linear fit), 0.06 (circles), 0.095 (diamonds), 0.25 (triangles); (right): $F_e/F_0 = 0.095$, top to bottom: $\omega = 0$ (squares), 10^{-3} (triangles), 10^{-2} (diamonds), 3×10^{-2} (circles), 10^{-1} (pluses).

by plotting

$$D^*(t') = [\sigma^2(t'+\tau) - \sigma^2(t')]/(2\tau). \qquad (18)$$

In settled "normal diffusion" regime this quantity must coincide (in average over the forcing period of duration τ) with the diffusivity, as in such a regime theoretically $\sigma^2(t+n\tau) = \sigma^2(t) + n\sigma^2(\tau)$ for $n \in \mathbb{N}$.

These results in part mean that the rule of superdiffusion or dispersionless stage (however these are modified in the high-frequency regime) terminating and turning into normal diffusion after one period of forcing no longer applies at high forcing frequencies. This leads to the $D(\omega)$ derivation based on approximations Eqs. (13,16) progressively less accurate at higher ω's, the power-law decay first slowing down, and then going into a completely different regime at ω approaching 2π.

At $\omega > 2\pi$ the diffusivity tends to the diffusivity of particles in the lattice periodic potential in the absence of extra driving $F_t(t)$. Such an asymptote is shown by the horizontal dot-dashed line in Fig. 6.

IV. DEPENDENCE OF DIFFUSIVITY ON TEMPERATURE AT FIXED FORCING FREQUENCY

Having studied how the temperature behavior of diffusion changes at gradual forcing frequency increase, here we investigate in more detail how the diffusivity changes with the temperature at fixed frequency. Besides theoretical importance, the results are of interest to experimentalists. Oftentimes changing the frequency in the system is problematic, while changing the temperatures is simpler; so the findings in this section are more straightforward to test.

Left part of Fig. 11 shows how the diffusivity changes with $T^\dagger$ at fixed $\omega = 10^{-2}$. For the forcing amplitude in region I the diffusivity monotonically grows with the temperature, this (normal) behavior agreeing with such at constant forcing [22]. For F_e in regions II and III TAD is observed, as already noted in Sec. III B–III C. TAD is confined to limited (from below) temperature intervals, contrary to the TAD behavior observed in [22] for constant forcing. In [22] the diffusivity was numerically checked growing (only in region II at $\omega = 0$) at temperature decreasing down to $T^\dagger = 0.097$. Such a behavior was understood theoretically, dependence $D \propto \exp[\mathcal{E}/(k_B T)]$ was predicted at low temperatures going all the way down to 0, and agreed well with simulation results.

In the current setup with periodic forcing, similar temperature dependence is observed too,

$$D \propto \exp(\epsilon_1/T^\dagger),\ \epsilon_1 > 0, \qquad (19)$$

but only above certain temperature. The growth slows down as the temperature keeps decreasing, D reaches maximum $D_{\max}(T_{\max})$ at certain $T_{\max}$, and starts decreasing with further decrease in T. The behavior at lower temperatures is well approximated by

$$D \propto \exp(-\epsilon_2/T^\dagger),\ \epsilon_2 > 0. \qquad (20)$$

In the absence of forcing we observe $\epsilon_2 = 1$ (corresponding dimensionful quantity $\mathcal{E}_2 = U_0$) — classical Arrhenius temperature behavior of the diffusivity. ϵ_2 decreases with F_e, whereas ϵ_1 increases. $T_{\max}$ and $D_{\max}$ increase with F_e as well.

Temperature behavior of the diffusivity is related to such of the superdiffusion stage duration $\tau_{\rm spd}$ and τ_1. These times may be inferred from simulations of the particle dispersion evolution with time, Fig. 12. For the

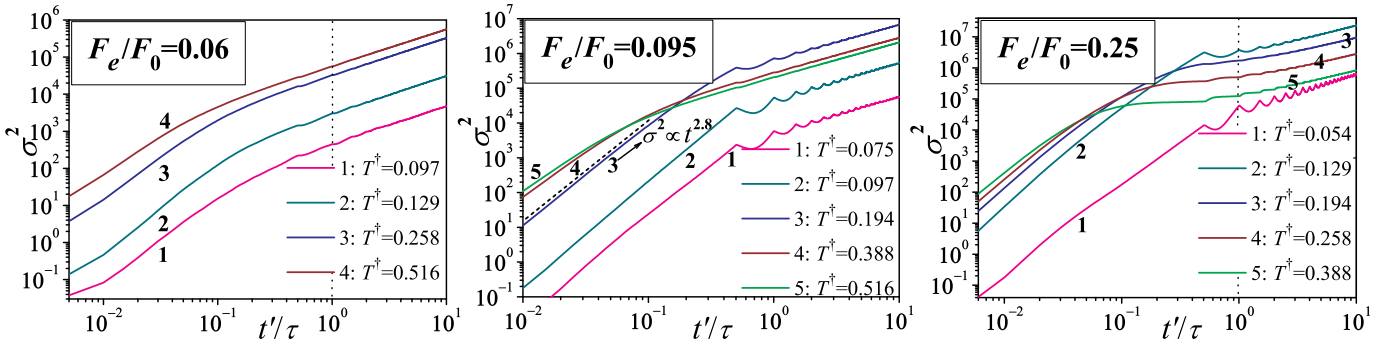

FIG. 12. (Color online) Dispersion of the particles as a function of time at different temperatures. Force amplitudes in regions I–III. $\omega = 10^{-2}$.

forcing amplitude in region I, τ_1 (the time at which superdiffusion starts, about the potential well escape time) increases with the temperature decreasing. $\tau_{\rm spd} = \tau_2 - \tau_1$ at the same time decreases. This is seen to result in the diffusivity growing with the temperature, agreeing with the results shown in the $\omega = 10^{-2}$ part of Fig. 11.

In region II τ_1 increases with the temperature decreasing as well. $\tau_{\rm spd}$ however also increases with the temperature decreasing (middle graph in Fig. 12, curves 3–5) — contrary to the behavior for F_e in region I. TAD is realized at these temperatures. At temperature $T_{\max}(F,\omega)$ ($T^\dagger \approx 0.194$ in this graph) τ_2 becomes equal to $\tau = 2\pi/\omega$, the period of forcing. At this temperature the maximal diffusivity is achieved, corresponding to the longest actual superdiffusion stage at the given forcing frequency. TAD is only realized at temperatures above $T_{\max}(F_e,\omega)$: even though $\tau_{\rm spd}$ (superdiffusion duration at constant forcing) still grows at further temperature decrease together with τ_2, in periodic forcing setup superdiffusion effectively ends earlier, at $t' \approx \tau$. It is this superdiffusion interruption at $t' \approx \tau$ that makes $D(T)$ behavior at lower temperatures to diverge in the periodic forcing setup from that at constant forcing. In the constant forcing problem, based on the same logic, TAD must be realized all the way down to $T = 0$; in agreement with conclusions in [22].

It is clear from this argument that there is no uniform convergence with ω of $D(T)|_\omega$ curves to $D(T)|_{F=const}$. At ω getting smaller $D(T)|_\omega$ gets close to such a $D(T)$ curve for constant forcing on longer T-interval, down to progressively lower temperatures. However at any ω there exists $T_{\rm TAD}(\omega)$ such that normal temperature dependence of the diffusivity is restored at $T < T_{\rm TAD}(\omega)$. This non-uniform convergence is shown in the right plot in Fig. 11.

The same behavior is observed in region III. The maximal diffusivity is achieved at $T_{\max}(F_e,\omega)$ corresponding to the longest superdiffusion stage at the given ω. The lowest temperature at which TAD is realized is the one at which τ_2 reaches the period of external force τ (more precisely, the time of superdiffusion interruption at a given ω). At this temperature $\partial D/\partial T|_{\{F_e,\omega\}=const}$ crosses zero value. The interval of temperatures, in which TAD is observed, is wider than at forcing in region II, due to the presence of dispersionless phase (curve 4 in the right plot in Fig. 12). Experimentally it is simpler to observe TAD at larger F_e, at which within the period of $F_t(t)$ the superdiffusion stage is used to larger extent; and the temperature interval of TAD is thus wider.

Presented study of the diffusion under external forcing can be summarized by the following schematics, Fig. 13. Force amplitudes fall into three regions, I–III. In region I the diffusivity grows with the temperature increasing. In regions II–III the dependence $D(T)$ is nonmonotonic, it shows a maximum at certain $T_{\max}$. Below $T_{\max}$ the temperature dependence of the diffusivity is normal, $\partial D/\partial T > 0$. Temperature interval of TAD exists above $T_{\max}$, $\partial D/\partial T < 0$.

In the forcing frequency dependence of the diffusivity, on the other hand, it is regions I and II that look alike: at the frequency decreasing from a fraction of the potential eigenfrequency the diffusivity grows monotonically, getting to a flat region at $\omega < \omega_2$, in which it virtually reaches its limiting $D(\omega = 0)$ value. In region III the $D(\omega)$ curve passes through a maximum, near $\omega = \omega_2 \equiv 2\pi/\tau_2$, corresponding to the end time of superdiffusion stage τ_2 at constant forcing. At frequencies getting smaller, the forcing period contains progressively longer interval of "would-be" (in the constant forcing problem) dispersionless and (at yet smaller frequencies) normal-diffusion time-interval, resulting in D decreasing at such further ω decrease.

V. SINUSOIDAL IN TIME EXTERNAL FORCING

Here we show the frequency dependence of the diffusivity for sinusoidal in time external forcing. We observe the same features in $D(\omega)$ as we saw for PCP forcing. Main conclusions of the sections above thus appear not to depend critically on specific form of time-dependence

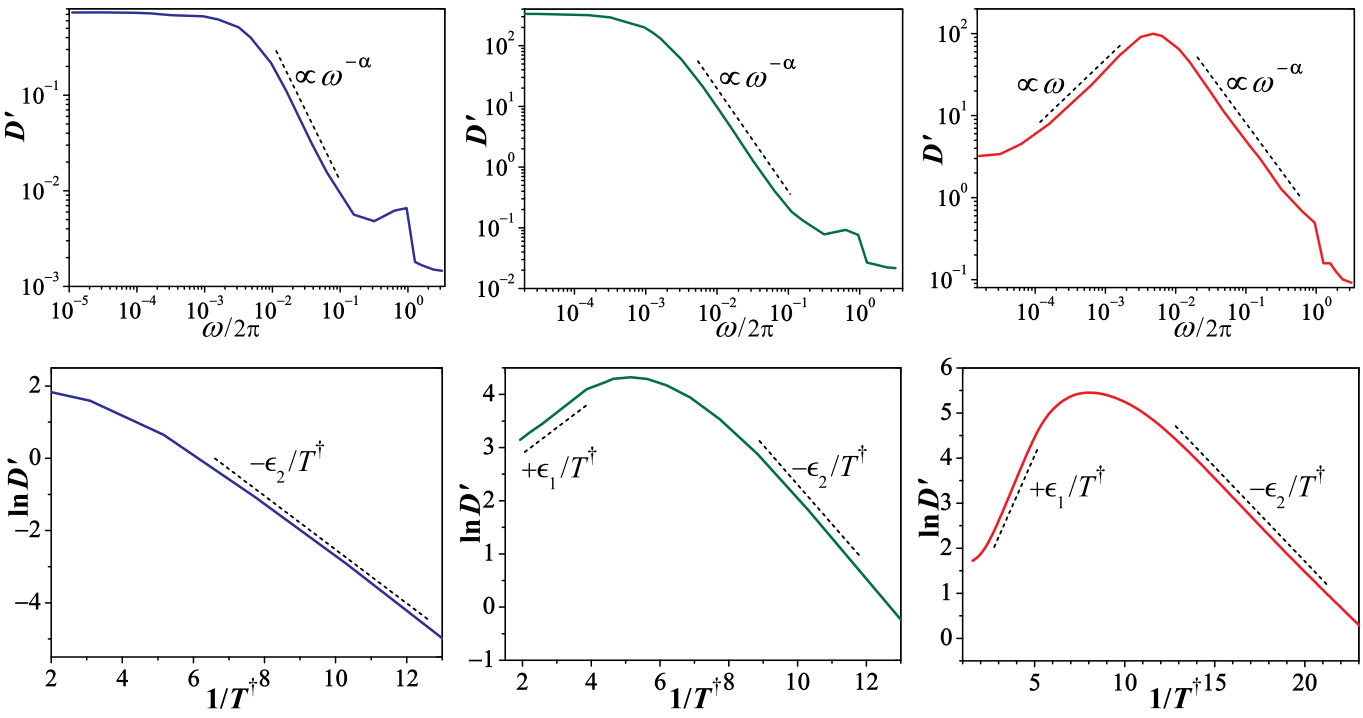

FIG. 13. (Color online) Features of the dependence of the diffusivity on the forcing frequency at fixed temperature (top) and on the inverse temperature at fixed frequency (bottom), for F_e in regions I–III.

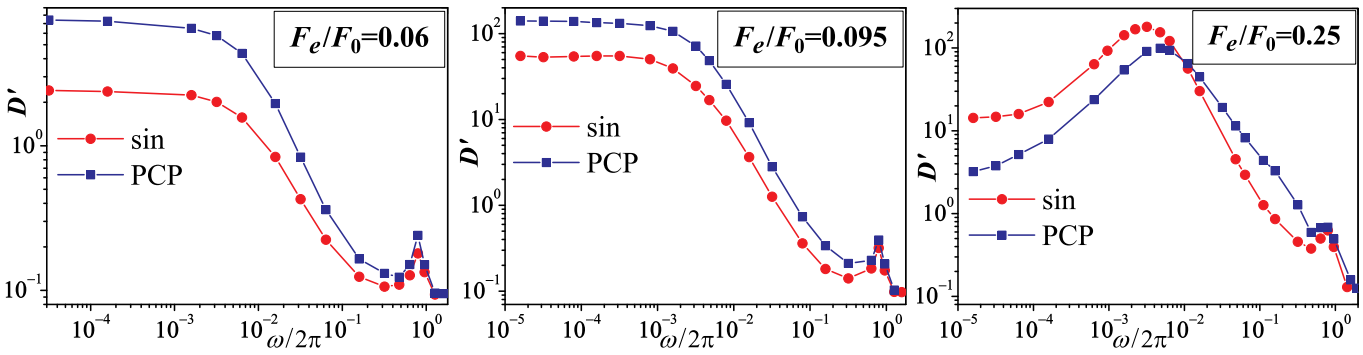

FIG. 14. (Color online) $D'(\omega)$ for force amplitude in regions I–III. $T^\dagger = 0.258$. Sinusoidal in time (circles) and PCP (squares) forcing.

of the (smooth enough, symmetric) forcing.

Figure 14 presents a comparison between diffusivities at sinusoidal in time and PCP forcing. At small frequencies the diffusivity stays close to its value at $\omega = 0$. In regions I and II of the external forcing amplitude $D(\omega)$ starts decaying according to a power law at $\omega > 2\pi/\tau_2$, τ_2 being the superdiffusion stage ending time at constant external forcing with the same amplitude F_e. In region III $D(\omega)$ grows linearly with ω at intermediate ω's, reaches a maximum, then shows a power-law decay at larger frequencies. For all force amplitudes the power law decay switches to more complex behavior at ω reaching about $1/10^{\text{th}}$ of the potential eigenfrequency.

Presence of periodic forcing of any form of time-dependence leads to significant enhancement in diffusivity. This enhancement is somewhat smaller for sinusoidal forcing in regions I, II (can be understood, as at the same F_e the average over period forcing $\langle|F_t|\rangle_t$ is smaller for sinusoidal than for PCP forcing). In region III the maximum in diffusivity is achieved at smaller $\omega_{\max}$, and the value of $D_{\max}$ is larger than such a maximal diffusivity at corresponding $\omega_{\max,\text{PCP}}$ under PCP driving with the same amplitude F_e. This can be understood from the same argument, as in region III the diffusivity *de-*

creases with the forcing increasing, all other parameters kept constant.

VI. CONCLUSIONS

We investigated enhancement of diffusion in 1D space-periodic underdamped systems by external time-periodic fields. We showed that the diffusion can be enhanced by orders of magnitude at certain choice of temperatures T, forcing amplitudes F_e and frequencies ω. Three regions of F_e exist, I–III, in which dependences of diffusivity D on T and ω differ qualitatively.

At all F_e there is an interval of small frequencies, in which D depends only weakly on the frequency, approaching the limiting value $D(\omega = 0)$. This value coincides with D at constant bias force with the same value F_e in the case of piecewise constant in time periodic (PCP) forcing, the form $F_t(t)$ of forcing we focused on in this study. At larger frequencies, from $\omega_2 = 2\pi/\tau_2$ corresponding to the superdiffusion stage ending time τ_2, to about $2\pi/10$ (dimensionful frequency $\Omega \approx 1/10^{\text{th}}$ of the potential eigenfrequency Ω_0) $D(\Omega)$ decays with Ω according to a power-law. The exponent of this decay is related to the superdiffusion stage exponent α. At yet larger frequencies non-equilibrium effects slow down the power-law decay of $D(\Omega)$, and, after a local maximum in $D(\Omega)$ near $\Omega \approx 0.8\Omega_0$, D tends to its asymptotic value coinciding with the diffusivity in the absence of external forcing.

At small forcing amplitudes, in regions I and II, $D(\Omega)$ decreases monotonically with frequency Ω from its value at constant forcing, all the way till the non-equilibrium effects become critical, at $\Omega \approx 0.3\Omega_0$. At stronger forcing, region III, $D(\omega)$ is nonmonotonic, a maximum is reached at $\omega_{\max} \approx \omega_2$. $D(\omega)$ grows monotonically on $\omega \in (0; \omega_{\max})$, this growth is approximately linear on certain interval to the left of ω_2.

We studied the temperature dependence of the diffusivity at fixed ω. Contrary to the constant forcing problem [22] the diffusivity increases with the temperature for all F_e when the temperature is below certain frequency-dependent threshold value. Limited temperature intervals exist for the force amplitudes in regions II and III, in which the diffusivity decreases with the temperature ("temperature-abnormal diffusivity", TAD).

The physical reason behind the strong diffusivity enhancement is emergence of two populations of particles under the action of external force, locked and running ones. At optimal F_e and T the number of particles in the two populations is comparable, long flights of the running particles relative to the locked population take place with significant probability, resulting in giant enhancement of diffusion.

For comparison we studied diffusivity under sinusoidal in time driving. We saw that the same features in $D(\omega)$ are observed in the three regions of force amplitudes as in PCP driving case. We thus conjecture that the qualitative features of $D(\omega, T, F_e)$ behavior are insensitive to specific functional dependence of the (symmetric, smooth enough in t) external force on time.

The effects investigated allow for simple experimental verification. Diffusion of particles on solid body surface is one natural arena for this. Such systems are characterized by low dissipation [36]. Another field to study TAD in is in propagation of magnetic particles on non-magnetic substrate, acted upon with electromagnetic fields. Abnormal diffusion enhancement could be manifested in, *e.g.*, enhanced growth of islands of the new phase at decreasing temperatures.

Once verified experimentally, the effect of abnormal diffusion enhancement can find applications in a number of new technologies: in sorting of particles, manufacturing surface structures with required properties, controlling penetration of particles through biological and artificial membranes, in memristors, devices with charge density waves, etc.

ACKNOWLEDGMENTS

We are grateful to Alexei Chechkin for useful discussions.

[1] H. Mehrer, *Diffusion in Solids* (Springer, Berlin, 2007).

[2] G. Antczak and G. Ehrlich, *Surface Diffusion* (Cambridge University Press, Cambridge, 2010); R. Dalbey, C. Koehler, and F. Tamanoi, eds., *Molecular Machines Involved in Protein Transport across Cellular Membranes*, The Enzymes, Vol. XXV (Elsevier, Amsterdam, 2007); S. Chakraborty, ed., *Microfluidics and Microfabrication* (Springer, New York, 2010).

[3] O. M. Braun and Yu. S. Kivshar, Physics Reports **306**, 1 (1998); C. Dalle-Ferrier, M. Krüger, R. D. L. Hanes, S. Walta, M. C. Jenkins, and S. U. Egelhaaf, Soft Matter **7**, 2064 (2011); I. Goychuk, Beilstein Journal of Nanotechnology **7**, 328 (2016), arXiv:1510.00422 [cond-mat.mes-hall]; F. Höfling and T. Franosch, Reports on Progress in Physics **76**, 046602 (2013), arXiv:1301.6990 [cond-mat.soft].

[4] P. Hänggi and F. Marchesoni, Reviews of Modern Physics **81**, 387 (2009), arXiv:0807.1283 [cond-mat.stat-mech].

[5] F. Evers, R. D. L. Hanes, C. Zunke, R. F. Capellmann, J. Bewerunge, C. Dalle-Ferrier, M. C. Jenkins, I. Ladadwa, A. Heuer, R. Castañeda-Priego, and S. U. Egelhaaf, European Physical Journal Special Topics **222**, 2995 (2013), arXiv:1308.5632 [cond-mat.soft].

[6] H. Risken, *The Fokker-Planck equation. Methods of solu-*

tion and applications (Springer, New York, 1989).
[7] S.-H. Lee and D. G. Grier, Physical Review Letters **96**, 190601 (2006), cond-mat/0603558.
[8] P. Tierno, P. Reimann, T. H. Johansen, and F. Sagués, Physical Review Letters **105**, 230602 (2010), arXiv:1012.3343 [cond-mat.stat-mech].
[9] P. Eshuis, K. van der Weele, D. Lohse, and D. van der Meer, Physical Review Letters **104**, 248001 (2010).
[10] S. Pagliara, C. Schwall, and U. F. Keyser, Advanced Materials **25**, 844 (2013).
[11] P. Sajeesh and A. K. Sen, Microfluidics and Nanofluidics **17**, 1 (2013).
[12] H. D. Vollmer and H. Risken, Zeitschrift fur Physik B Condensed Matter **34**, 313 (1979); H. Risken and H. D. Vollmer, Zeitschrift fur Physik B Condensed Matter **33**, 297 (1979).
[13] H. Risken and H. D. Vollmer, Physics Letters A **69**, 387 (1979); Zeitschrift fur Physik B Condensed Matter **35**, 177 (1979); H. D. Vollmer and H. Risken, Zeitschrift fur Physik B Condensed Matter **37**, 343 (1980); P. Jung and H. Risken, Zeitschrift fur Physik B Condensed Matter **54**, 357 (1984).
[14] G. Costantini and F. Marchesoni, EPL (Europhysics Letters) **48**, 491 (1999).
[15] H. Gang, A. Daffertshofer, and H. Haken, Physical Review Letters **76**, 4874 (1996); M. Borromeo, G. Costantini, and F. Marchesoni, Physical Review Letters **82**, 2820 (1999).
[16] K. Lindenberg, J. M. Sancho, A. M. Lacasta, and I. M. Sokolov, Physical Review Letters **98**, 020602 (2007), cond-mat/0612047; J. M. Sancho, A. M. Lacasta, K. Lindenberg, I. M. Sokolov, and A. H. Romero, Physical Review Letters **92**, 250601 (2004), cond-mat/0310589.
[17] M. Khoury, J. P. Gleeson, J. M. Sancho, A. M. Lacasta, and K. Lindenberg, Phys. Rev. E **80**, 021123 (2009).
[18] K. Lindenberg, A. M. Lacasta, J. M. Sancho, and A. H. Romero, New Journal of Physics **7**, 29 (2005).
[19] P. Reimann, C. van den Broeck, H. Linke, P. Hänggi, J. M. Rubi, and A. Pérez-Madrid, Physical Review Letters **87**, 010602 (2001); Phys. Rev. E **65**, 031104 (2002).
[20] B. Lindner, M. Kostur, and L. Schimansky-Geier, Fluctuation and Noise Letters **1**, R25 (2001).
[21] E. Heinsalu, R. Tammelo, and T. Örd, Physica A Statistical Mechanics and its Applications **340**, 292 (2004
[22] I. G. Marchenko, I. I. Marchenko, and A. V. Zhiglo, European Physical Journal B **87**, 10 (2014).
[23] M. Evstigneev, O. Zvyagolskaya, S. Bleil, R. Eichhorn, C. Bechinger, and P. Reimann, Phys. Rev. E **77**, 041107 (2008).
[24] X.-g. Ma, P.-Y. Lai, B. J. Ackerson, and P. Tong, Soft Matter **11**, 1182 (2015).
[25] I. G. Marchenko and I. I. Marchenko, EPL (Europhysics Letters) **100**, 50005 (2012).
[26] U. Bovensiepen, H. Petek, and M. Wolf, eds., *Dynamics at Solid State Surfaces and Interfaces*, Vol. 1 (Wiley-VCH, Weinheim, 2010); D. Woodruff, ed., *The Chemical Physics of Solid Surfaces: Surface Dynamics* (Elsevier, Amsterdam, 2003).
[27] A. Kulemin, *Ultrasound and diffusion in metals* (Metallurgy, Moscow, 1978) in Russian.
[28] D. Speer, R. Eichhorn, and P. Reimann, EPL (Europhysics Letters) **97**, 60004 (2012), arXiv:1203.2751 [cond-mat.stat-mech].
[29] J. M. Sancho and A. M. Lacasta, European Physical Journal Special Topics **187**, 49 (2010).
[30] I. G. Marchenko and I. I. Marchenko, Soviet Journal of Experimental and Theoretical Physics Letters **95**,
[31] I. G. Marchenko and I. I. Marchenko, Journal of Physics Conference Series **514**, 012045 (2014).
[32] A. M. Lacasta, J. M. Sancho, A. H. Romero, I. M. Sokolov, and K. Lindenberg, Phys. Rev. E **70**, 051104 (2004), cond-mat/0407781.
[33] D. Kuznetsov, *Stochastic differential equations: theory and practice of numerical solution* (St. Petersburg Polytech. Univ. Press, St. Petersburg, 2010) in Russian.
[34] B. Lindner and E. M. Nicola, Physical Review Letters **101**, 190603 (2008).
[35] S. Saikia and M. C. Mahato, Phys. Rev. E **80**, 062102 (2009), arXiv:0908.1024 [cond-mat.stat-mech].
[36] L. W. Bruch, R. D. Diehl, and J. A. Venables, Reviews of Modern Physics **79**, 1381 (2007); J. Krim, Advances in Physics **61**, 155 (2012).